Chemistry & Biology
Article

# DKxanthene Biosynthesis—Understanding the Basis for Diversity-Oriented Synthesis in Myxobacterial Secondary Metabolism

Peter Meiser,[1] Kira J. Weissman,[1] Helge B. Bode,[1] Daniel Krug,[1] Jeroen S. Dickschat,[1,2] Axel Sandmann,[1] and Rolf Müller[1,*]
[1]Institut für Pharmazeutische Biotechnologie, Saarland University, P.O. Box 151150, 66041 Saarbrücken, Germany
[2]Present address: Institut für Organische Chemie, Technical University of Braunschweig, 38106 Braunschweig, Germany
*Correspondence: rom@mx.uni-saarland.de
DOI 10.1016/j.chembiol.2008.06.005

## SUMMARY

**The DKxanthenes are a family of yellow pigments which play a critical role in myxobacterial development. Thirteen unique structures from *Myxococcus xanthus* DK1622 differ in the length of their characteristic polyene functionality, as well as the extent of methyl branching. We aimed to understand the mechanistic basis for this "molecular promiscuity" by analyzing the gene cluster in DK1622, and comparing it to the DKxanthene biosynthetic locus in a second myxobacterium, *Stigmatella aurantiaca* DW4/3-1, which produces a more limited range of compounds. While the core biosynthetic machinery is highly conserved, *M. xanthus* contains a putative asparagine hydroxylase function which is not present in *S. aurantiaca*. This observation accounts, in part, for the significantly larger metabolite family in *M. xanthus*. Detailed analysis of the encoded hybrid polyketide synthase (PKS)-nonribosomal peptide synthetase (NRPS) assembly line provides direct evidence for the mechanism underlying the variable polyene length and the observed pattern of methyl functionalities.**

## INTRODUCTION

The DKxanthenes comprise a novel family of secondary metabolites that are characteristic of the Gram-negative soil-dwelling bacterium *Myxococcus xanthus* (Meiser et al., 2006; Krug et al., 2008). The presence of such pigments in *M. xanthus* was suspected for decades, because growth phase cells give rise to bright yellow colonies (Burchard et al., 1977). Natural so-called "phase variants" of *M. xanthus* exhibit a paler, tan phenotype, indicative of a deficiency in pigment production. In addition, tan cells are unable to form mature myxospores, supporting a role for the DKxanthenes in regulating the complex life cycle of the myxobacteria (Laue and Gill, 1994, 1995; Kaiser, 2004; Kuner and Kaiser, 1982; Shimkets, 1999). Indeed, deliberate inactivation of the DKxanthene biosynthetic pathway resulted in tan-colored mutants that were defective in both fruiting body formation and sporulation (Meiser et al., 2006), suggesting that the natural phase variants exhibit the same deficit. Furthermore, these defects could be at least partially complemented by the addition of purified DKxanthenes (Meiser et al., 2006). Nonetheless, the precise role that the DKxanthenes play in morphological differentiation remains to be elucidated.

"Retrobiosynthetic analysis" of the DKxanthenes strongly suggested their origin from a hybrid polyketide synthase (PKS)-nonribosomal polypeptide synthetase (NRPS) system, an expectation that was confirmed by identification of the gene cluster (Meiser et al., 2006). PKSs and NRPSs are gigantic multienzyme "assembly lines" that catalyze the sequential condensation of simple building blocks, acyl-CoA thioesters and amino acids, respectively (Walsh, 2008; Weissman and Leadlay, 2005). Chain extension is accomplished by successive modules of enzymes, and thus, the genetic organization is colinear with the sequence of biosynthetic transformations. PKS modules minimally incorporate acyl transferase (AT) and ketosynthase (KS) domains, which are required for selection of a specific building block and its incorporation via a thioclaisen-like condensation, into the growing chain. The resulting intermediate can undergo a variable extent of redox adjustment, depending on the specific complement of reductive domains (ketoreductase [KR], dehydratase [DH], and enoyl reductase [ER]) present within the module. Throughout the biosynthesis, the chain extension intermediates are tethered to the multienzymes in thioester linkage to the phosphopantetheine prosthetic group of the integral acyl carrier protein (ACP) of each module; this architecture allows the chains to be shuttled efficiently between the various active sites. The analogous core functions of NRPSs include condensation (C) (or heterocyclization [HC]) and PCP domains, whereas optional modifying enzymes may comprise epimerase (E), methyl transferase (MT), and oxidase (Ox) functions (Walsh et al., 2001). Chain termination in both systems is typically performed by an integral thioesterase (TE) activity (Kopp and Marahiel, 2007). The existence of hybrid PKS-NRPS multienzymes reflects the shared biosynthetic logic of the two systems.

The modular organization of PKSs and NRPSs has encouraged efforts to engineer these systems to produce new structures with potential as drug leads (Walsh, 2008; Weissman and Leadlay, 2005). Although genetic manipulation, particularly of PKS systems, has been demonstrated to yield the expected products, the low efficiency of these experiments has so far limited their use in industrial drug discovery and has highlighted the

A

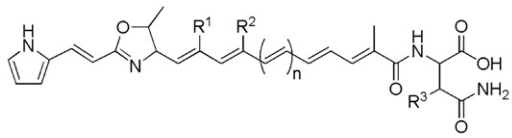

| *M. xanthus* | | n | $R^1$ | $R^2$ | $R^3$ | *S. aurantiaca* |
|---|---|---|---|---|---|---|
| • | DKxanthene-492 | 1 | $CH_3$ | H | H | |
| • | DKxanthene-504 | 2 | H | H | H | • |
| • | DKxanthene-508 | 1 | $CH_3$ | H | OH | |
| ● | DKxanthene-518 | 2 | $CH_3$ | H | H | ● |
| • | DKxanthene-520 | 2 | H | H | OH | |
| • | DKxanthene-530 | 3 | H | H | H | • |
| ● | DKxanthene-534 | 2 | $CH_3$ | H | OH | |
| • | DKxanthene-544 | 3 | $CH_3$ | H | H | ● |
| ● | DKxanthene-548 | 2 | $CH_3$ | $CH_3$ | OH | |
| • | DKxanthene-556 | 4 | H | H | H | • |
| ● | DKxanthene-560 | 3 | $CH_3$ | H | OH | |
| • | DKxanthene-574 | 3 | $CH_3$ | $CH_3$ | OH | |
| • | DKxanthene-586 | 4 | $CH_3$ | H | OH | |

B

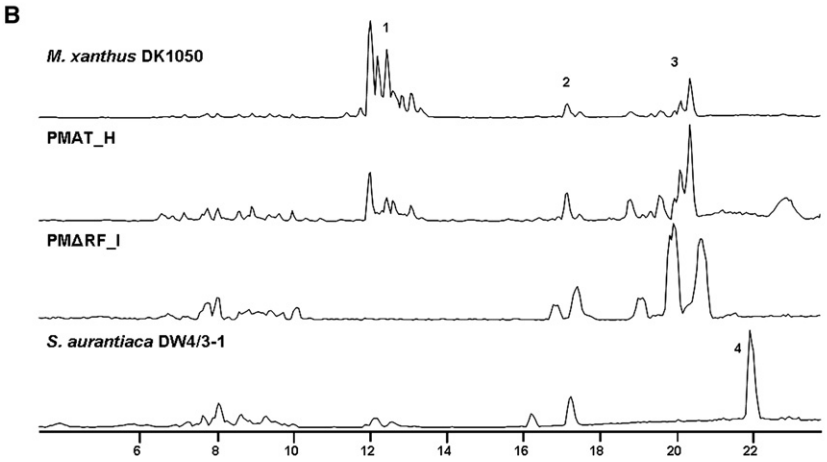


**Figure 1. The DKxanthene Metabolite Families and HPLC-MS Analysis of Strains in this Study**

(A) DKxanthenes structures present in *M. xanthus* DK 1622/1050 and *S. aurantiaca* DW4/3-1. The relative quantity of each metabolite is indicated by the dot intensity. n indicates both the number of double bonds at this position, as well as the number of iterations required to generate the observed polyene.

(B) HPLC-MS analysis of *M. xanthus* and *S. aurantiaca* wild-type strains, as well as *M. xanthus* mutants PMAT_H and PMΔRF_I. Wild-type *M. xanthus* produces the DKxanthenes (1) as the major metabolites. AT domain mutant PMAT_H produces the same range of compounds as wild-type *M. xanthus* but at lower yields. Production of DKxanthenes by the mutant PMΔRF_I is abolished, the same phenotype observed with all other KR mutants. The DKxanthenes are produced as minor metabolites by wild-type *S. aurantiaca*, with cultures extracts dominated by myxothiazol (4). Further metabolites include the lipid species lysophosphatidylethanolamine (2) (Avadhani et al., 2006) and the myxalamids and myxovirescins (3).

need to improve our fundamental understanding of the structure and function of these gigantic proteins (Weissman and Müller, 2008b). The DKxanthene biosynthetic pathway represents an attractive target for investigation because it incorporates both PKS and NRPS machineries. Furthermore, although modular megasynthases in *Streptomyces* typically generate one or a few closely related metabolites, the DKxanthene pathway gives rise to a suite of structural variants (Weissman and Müller, 2008a; Fischbach and Clardy, 2007). Even more remarkably, 37 epothilones are produced by a single strain of *Sorangium cellulosum* (Hardt et al., 2001). We aimed to shed light on the molecular basis for this "diversity-oriented biosynthesis," which is common to many myxobacteria, by analyzing the DKxanthene biosynthetic genes. Here, we report a detailed analysis of the cluster in the model strain *M. xanthus* DK1622 and compare it to a second, novel DKxanthene locus in the myxobacterium *Stigmatella aurantiaca* DW4/3-1. These data reveal an unusual biosynthetic pathway that makes variable use of a highly iterative PKS module.

## RESULTS AND DISCUSSION

### DKxanthene Production in *Myxococcus xanthus* DK1050/DK1622 and *Stigmatella aurantiaca* DW4/3-1

Eleven unique DKxanthene derivatives were recently identified in extracts of *M. xanthus* strains DK1050 and DK1622 (Meiser et al., 2006), with evidence for several additional metabolites. The structures range in mass from 492 to 586 Da and differ in overall chain length, extent of methyl branching, and modification of the terminal asparagine residue by hydroxylation (Figure 1A). DKxanthenes −518, −534, and −560 have been detected in all 98 strains of *M. xanthus* investigated to date (Krug et al., 2008), consistent with their essential role in cellular differentiation. Screening for secondary metabolites in other myxobacterial species revealed the presence of DKxanthenes in extracts of *Stigmatella aurantiaca* DW4/3-1; in this strain, the DKxanthenes represent minor metabolites, as myxothiazol constitutes the major product (Figure 1B). Many of the DW4/3-1 DKxanthenes (−504, −518, and −545; Figure 1A) had previously been identified in *M. xanthus* DK1050. However, two novel derivatives were detected that carry a proton at position $R^1$, a structural variation present in the known *M. xanthus* metabolites DKxanthene −504 and −520. Both of the novel compounds, DKxanthene −530 and −556, were subsequently identified as minor components in extracts of *M. xanthus* DK1050, bringing the total number of family members in the strain to 13. Additionally, we observed two compounds in DW4/3-1 with the same masses as DKxanthene −548 and −574 but whose retention times and fragmentation patterns differed, suggesting that the structures are also novel.

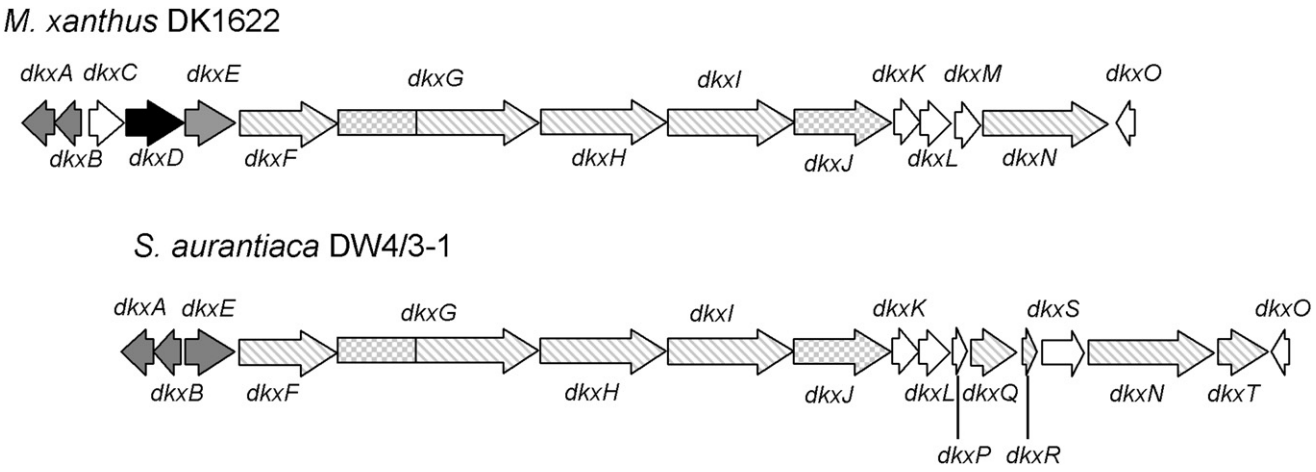


**Figure 2. The DKxanthene Biosynthetic Gene Clusters of *M. xanthus* DK1622 and *S. aurantiaca* DW4/3-1**

Schematic representation of the DKxanthene biosynthetic loci in *M. xanthus* and *S. aruantiaca*: dark gray, genes involved in starter unit biosynthesis; hatched, PKS genes; checkered, NRPS genes; black, putative hydroxylase; and white, genes of unknown function. The *S. aurantiaca* cluster lacks *dkxC* and *dkxD* relative to *M. xanthus* but incorporates additional genes, including discrete PKS domains (see also Tables 1 and 2).

## Identification and Analysis of the DKxanthene Biosynthetic Gene Clusters in *M. xanthus* and *S. aurantiaca* DW4/3-1

The complete genome sequence of *M. xanthus* DK1622 was published recently (Goldman et al., 2006). However, the strain exhibits yellow/tan phase variation (Ruiz-Vazquez and Murillo, 1984), which we anticipated would complicate the analysis of insertional mutagenesis experiments designed to identify the DKxanthene biosynthetic locus. We therefore located the gene cluster in *M. xanthus* strain DK1050, a stable yellow variant of the shared parental strain, *M. xanthus* FB (Ruiz-Vazquez and Murillo, 1984). DK1050 and DK1622 produce the same spectrum of DKxanthene derivatives in the same proportions, strongly supporting the equivalency of the gene clusters in the two strains. The DKxanthene cluster in DK1050 was identified by pMycoMar-based transposon mutagenesis, as described elsewhere (Sandmann et al., 2004): tan colonies were isolated and the transposon insertion site was identified by vector recovery from genomic DNA. Sequenced fragments of the cluster in DK1050 were then used in BLAST (Altschul et al., 1997) analysis against the DK1622 genome sequence. The DK1622 cluster ($dkx_{DK}$; Figure 2) occupies approximately 48 kbp of the genome and exhibits an average GC content of 69%, which is characteristic of myxobacteria. The DKxanthene cluster in *S. aurantiaca* DW4/3-1 was identified using sequence information from two neighboring but nonoverlapping contigs from the unfinished genome sequence of this strain and sequencing of the missing region in gene *dkxS*. The identity of the cluster was then confirmed by insertional mutagenesis within the KS domain of *dkxG*, which resulted in a DKxanthene-negative phenotype (Table S1, available online). The cluster in *S. aurantiaca* ($dkx_{DW}$) is approximately 51 kbp in size, with an overall GC content of 65%.

The complement of core biosynthetic genes in each species is the same, and the corresponding genes exhibit high sequence identity (Table S2), suggesting a common evolutionary origin for the two clusters. The shared genes encode enzymes for starter unit selection and modification (*dkxA*, *dkxB*, and *dkxE*), four PKS multienzymes (*dkxF*, *dkxH*, *dkxI*, and *dkxN*), an NRPS (*dkxJ*), and a hybrid PKS-NRPS subunit (*dkxG*) (Figure 2 and Table 1). The DKxanthene biosynthetic gene cluster in DW4/3-1 lacks the *M. xanthus* genes *dkxC* and *dkxD*, however, which are homologs of type I phosphodiesterases and FAD-dependent monooxygenases, respectively (Table 2). Genes *dkxP*, *dkxQ*, *dkxR*, *dkxS*, and *dkxT* are present in *S. aurantiaca* but are missing in the *M. xanthus* cluster (Tables 1 and 2). One possible explanation for the observed architectures is that both gene clusters evolved from a common ancestor by gene insertion (in the *dkxB*/*dkxE* intergenic region in the case of *M. xanthus*, and into both the *dkxL*/*dkxN* and *dkxN*/*dkxO* intergenic regions of *S. aurantiaca*).

## Determining the Order of PKS and NRPS Subunits in the DKxanthene Assembly Line

In many systems of Streptomycete origin, the sequence of the biosynthetic proteins within the pathway directly correlates with the order of the genes within the cluster. This colinearity is not observed, however, in the DKxanthene clusters. Gene *dkxN*, whose involvement in the pathway was demonstrated by insertional mutagenesis, is located downstream of gene *dkxJ* in both the $dkx_{DK}$ and $dkx_{DW}$ loci. Multienzyme DkxJ incorporates a terminal thioesterase domain and so is likely to be the last subunit in the pathway. We assumed, however, that the remaining genes were present in the appropriate order; thus, we aimed to localize multienzyme DkxN among the other subunits.

The assumption of genetic noncolinearity was supported by analysis of the "docking domains" present on each of the encoded multienzymes, which additionally aided in defining the correct start codon for each polypeptide. Docking domains are short sequence elements, located at both the C and N termini of the proteins, which mediate specific recognition between successive subunits within the synthetases (Richter et al., 2008). Sequence analysis has identified two groups of docking domains within mixed PKS-NRPS. The first operates at PKS-PKS junctions, whereas the second functions at either PKS-NRPS or

**Table 1. Proteins Involved in PKS/NRPS Biochemistry in DKxanthene Biosynthesis in *M. xanthus* DK1622 and *S. aurantiaca***

| Protein/Gene | Length (bp/aa) | Description | Module | Domains (Position in Protein [aa]) |
|---|---|---|---|---|
| DkxA/*dkxA* | 1515/504 | L-prolyl-AMP-ligase | M1 | A1 (155–372) |
| DkxB/*dkxB* | 1140/279 | L-prolyl-S-PCP Dehydrogenase | M1 | |
| DkxE/*dkxE* | 2211/736 | | M1 | KS1 (4–428) PCP1 (613–680) |
| DkxF/*dkxF* | 4266/1421 | PKS | M2 | KS2 (37–463) AT2 (576–764) KR2 (1051–1228) ACP2 (1330–1396) |
| DkxG/*dkxG* | 8922/2973 | NRPS/PKS | M3 | HC3 (69–554) A3 (679–893) PCP3 (1061–1125) |
| | | | M4 | KS4 (1053–1574) AT4 (1681–1975) DH4 (2039–2212) KR4 (2586–2763) ACP4 (2858–2925) |
| DkxH/*dkxH* | 5562/1854 | PKS | M5 | KS5 (38–463) AT5 (569–861) DH5(923–1100) KR5 (1460–1637) ACP5 (1737–1804) |
| DkxI/*dkxI* | 5490/1829 | PKS | M6 | KS6 (33–457) AT6 (559–853) DH6 (922–1091) KR6 (1457–1635) ACP6 (1758–1802) |
| DkxJ/*dkxJ* | 4308/1435 | NRPS | M7 | C7 (74–504) A7 (676–888) PCP7 (1054–1118) TE (1146–1404) |
| DkxN/*dkxN* | 5559/1852 | PKS | M8 | KS8 (39–467) AT8 (573–571) DH8 (941–1111) KR8 (1468–1646) ACP8 (1738–1805) |
| DkxO/*dkxO* | 789/262 | TE | M9 | TE (26–254) |
| DkxQ/*dkxQ*[a] | 2334/778 | PKS | | KR (580–737) |
| DkxR/*dkxR*[a] | 627/209 | PKS | | ACP (126–193) |
| DkxT/*dkxT*[a] | 2850/950 | PKS | | KS (33–458) AT (563–849) |

[a] The indicated data correspond to the *M. xanthus* DKxanthene biosynthetic gene cluster, with the exception of proteins DkxQ, DkxR, and DkxT which are present only in *S. aurantiaca*.

NRPS-NRPS interfaces; presumptive docking domains, which occur at NRPS-PKS junctions, do not exhibit obvious mutual sequence similarities (Weissman and Müller, 2008a). The existence of multiple, inherently orthogonal sets of docking elements is assumed to play a crucial role in ensuring the correct ordering of subunits within the assembly lines (Richter et al., 2008). The NMR solution structure of a representative NRPS N-terminal docking domain was solved recently (Richter et al., 2008). The domain adopts a novel αββαα fold featuring an exposed β-hairpin, which serves as the binding site for the partner docking

**Table 2. Predicted Functions of Non-PKS/NRPS Proteins Present in the DKxanthene Biosynthetic Gene Clusters of *M. xanthus* and *S. aurantiaca***

| Protein/ Gene | Length (bp/aa) | Putative Function/ Homolog | Origin | Similarity/ Identity, (%) | Accession Number of the Protein Homolog |
|---|---|---|---|---|---|
| DkxC/*dkxC*[a] | 1386/462 | Type 1 phosphodiesterase | *Nodularia spumigena* CCY9414 | 74/49 | ZP_016285151 |
| DkxD/*dkxD*[a] | 2544/847 | FAD-dependent monooxygenase | *Herpetosiphon aurantiacus* ATCC 23779 | 58/38 | YP_001544272 |
| DkxK/*dkxK* | 1059/352 | Phospholipase, patatin family | *Angiococcus disciformis* | 49/33 | CAF05653 |
| DkxL/*dkxL* | 1164/387 | Arsenite-acitvated ATPase ArsA | *Solibacter usitatus* Ellin6076 | 57/33 | YP_827141 |
| DkxP/*dkxP*[b] | 399/133 | No homology | | | |
| DkxM/*dkxM* | 471/156 | No homology | | | |
| DkxS/*dkxS*[b] | 1878/626 | Radical SAM domain protein | *Solibacter usitatus* Ellin6076 | 58/40 | YP_822161 |

The data shown correspond to the *M. xanthus* DKxanthene biosynthetic gene cluster, if not otherwise indicated.
[a] ORF present only in *M. xanthus* DK1622.
[b] ORF present only in *S. aurantica* DW4/3-1.

domain. The pattern of solvent-accessible charged residues on the β sheet appears to define an electrostatic "code" for docking at this type of interface.

Consistent with our proposed order, the docking domains at the DkxI/DkxJ junction show convincing homology to other docking elements that operate at PKS-NRPS interfaces from a range of systems; the positive charges of the putative code residues on DkxJ (two Arg) are complemented by a negative charge cluster on the upstream partner DkxI (two Glu) (Figure S1). The C-terminal docking domain of PKS DkxF, which should also interact with an NRPS docking domain, does not exhibit strong homology to the DkxI sequence group (Figure S1); however, it contains a charge cluster in an equivalent position, but whose polarity is reversed (Lys, Arg). Correspondingly, several solvent-accessible residues on the presumptive β sheet of DkxG are negatively charged. Furthermore, the N-terminal docking domains of DkxF, H, N, and I cluster with other docking domains from PKS-PKS junctions, as do the C-terminal docking domains of DkxE, G, H, and N. However, the docking elements show enough sequence variability, particularly among the N-terminal domains (Figure S1), to support their role as specificity determinants. Taken together with the mechanistic requirements of the pathway, these considerations narrowed the possible locations of subunit DkxN to positions downstream of either DkxG or DkxH (Figure 2).

The gene cluster in *S. aurantiaca* contains three additional PKS genes relative to that of *M. xanthus*, *dkxQ* encoding a discrete KR domain, *dkxR* encoding a standalone ACP, and *dkxT* encoding a KS-AT didomain, which together could form a functional module; such "split module" organization has precedence in mixed assembly lines from myxobacteria, *Bacillus* species, and other bacteria (Julien et al., 2006; Perlova et al., 2006; Kopp et al., 2005; Simunovic et al., 2006; Chen et al., 2006; Butcher et al., 2007; Silakowski et al., 2001). However, the gene complement in *M. xanthus* is sufficient to generate the full range of DKxanthenes observed in *S. aurantiaca*, and so such an additional module is not required for the biosynthesis. Indeed, inspection of the AT domain of DkxT shows that it contains mutations in two active site residues ($Ser_{91}$ and $H_{201}$, numbered according to Yadav et al., 2003), and so is unlikely to be active.

## Biosynthesis of the DKxanthene Backbones

Unless specified otherwise, the following discussion will refer to the DKxanthene pathway in *M. xanthus* DK1622, because that in *S. aurantiaca* DW4/3-1 is expected to be the same (mutual sequence identity between all proteins is greater than 64%; Table S2). We hypothesized that the starter unit incorporated into the DKxanthenes was likely to be pyrrole carboxylic acid, a building block that is present in several other natural products of bacterial origin, including pyoluteorin (Thomas et al., 2002) and coumermycin $A_1$ (Xu et al., 2002; Garneau et al., 2005). In these pathways, L-proline is activated as its adenylate by a free-standing A domain (PltF [pyoluteorin] and ProB [coumermycin A1], respectively), and transferred to a discrete PCP (PltE; ProA), thereby sequestering the amino acid from primary metabolism. The carrier protein-bound residue then undergoes a four-electron oxidation catalyzed by a novel class of flavoprotein dehydrogenases (PltL; ProC), to afford the pyrrole-2-carboxylate. The resulting thioester species is activated as an acyl donor for subsequent reactions. Inspection of the gene complement in the DKxanthene cluster suggests that the pathway uses a similar strategy to divert proline into secondary metabolism. Clear homologs for both the adenylation and dehydrogenase activities are present in the cluster —DkxA and DkxB, respectively (45%–49% identity on the protein level). However, the cluster does not contain a discrete ACP domain analogous to PltE and ProA. Instead, the activated prolyl-AMP is likely to be thioesterified directly onto the ACP domain of the unusual didomain KS-ACP loading module, DkxE (Figure 3). Consistent with the nonessential nature of the KS domain for the biosynthesis, sequence analysis suggests that the domain is inactive, because it exhibits significant deviations from typical KS active site motifs (e.g., substitution of an essential His by Tyr) (Table S3).

To provide support for this proposal, the A domain homolog *dkxA* was inactivated by plasmid insertion in *M. xanthus*. As anticipated, the resulting mutant PM1284 exhibited a DKxanthene-negative ($Dkx^-$) phenotype. Production of the DKxanthenes could be restored to 25% of wild-type level by administration of *N*-acetyl-*S*-pyrrolyl-2-carboxylcysteamine (pyrrolyl-2-carboxyl-SNAC) to cultures of PM1284. However, alternative substrates including the NAC thioesters of benzoic acid and nicotinic acid were not accepted (data not shown). Reconstitution in this case presumably arose from recognition of pyrrolyl-2-carboxyl-SNAC as an analog of the ACP-bound thioester, strongly supporting the involvement of the pyrrolyl-2-carboxyl-ACP in the pathway (Figure 3B). Taken together, these data bolster the proposal that biosynthesis of mono-pyrrolic natural products in microbes occurs by a common molecular logic, in which carrier proteins are used as a device for substrate channeling (Walsh et al., 2006).

The first round of chain extension occurs with condensation of pyrrolyl-2-carboxylate with malonate, catalyzed by the PKS module DkxF. DkxF exhibits several unusual features relative to "classical" PKS modules. For example, the AT domain shows only weak homology to other PKS AT domains, and the active site Ser residue appears to be absent. Other PKS systems, such as those responsible for biosynthesis of aureothin (He and Hertweck, 2005), pyoluteorin (Nowak-Thompson et al., 1997, 1999), and neocarzilin (Otsuka et al., 2004), contain similarly aberrant and, presumably, nonfunctional AT domains. In the case of aureothin, the affected module has nonetheless been shown to participate in chain extension (He and Hertweck, 2005). As with DKxanthene biosynthesis, the basis for complementation of the AT activities remains unknown, but presumably malonate is furnished to the ACP domain by a discrete AT domain acting in *trans*. Module DkxF also lacks an integral DH domain required to generate the double bond observed in the DKxanthene metabolite family. As postulated for other myxobacterial PKS, the functions of the missing DHs may be complemented by the iterative action of a DH domain located in a downstream module (Perlova et al., 2006; Frank et al., 2007; Tang et al., 2004), or by a discrete DH domain encoded elsewhere in the genome. Alternatively, formation of the stable, conjugated system may not require specific catalysis. Biosynthesis continues with a switch to NRPS logic. The next building block incorporated into the DKxanthenes is L-threonine, as demonstrated by feeding studies using [$^{13}C$, $^{15}N$]-labeled amino acid

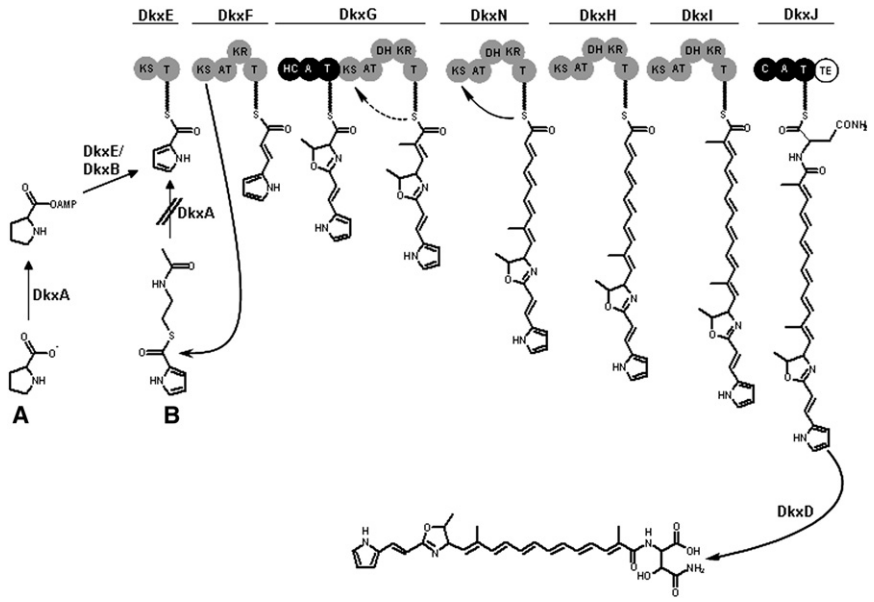


**Figure 3. Model for DKxanthene Biosynthesis, Shown for the Major Metabolite DKxanthene −534 in *M. xanthus* DK1622**

(A) Biosynthesis is initiated by transfer of L-proline to the ACP of subunit DkxE by the A domain DkxA, followed by DkxB-catalyzed dehydrogenation to afford pyrrole-2-carboxylate.

(B) Inactivation of gene *dkxA* leads to DKxanthene-negative mutants; production is restored by administration of pyrrolyl-2-carboxyl-SNAC. The biosynthetic position of DkxN in the assembly line is suggested by analysis both of the cluster architecture and of putative "docking domains." However, we cannot at present exclude an alternative module ordering, in which subunits DkxN and DkxH are reversed. The solid curved arrow indicates the proposed iterative behavior of DkxN, which gives rise to the polyene of DKxanthene −534. Our data also provide direct evidence for iteration by the PKS module of DkxG (dotted curved arrow), in the biosynthesis of other DKxanthene metabolites. PKS portion (light gray): KS, ketosynthase; AT, acyl transferase; KR, ketoreductase; DH, dehydratase; and T, thiolation (acyl carrier protein). NRPS portion (black): HC, heterocyclization; A, adenylation; T, thiolation (peptidyl carrier protein); and C, condensation domain. TE (white), thioesterase.

(Meiser et al., 2006). Cyclization of threonine by the N-terminal HC domain affords the 5-methyloxazoline moiety.

Together, the next four PKS modules install the characteristic polyene functionality of the DKxanthenes. According to "textbook" rules for biosynthesis on modular multienzymes, each module catalyzes a single round of chain extension. However, inspection of the cluster reveals that the 4 PKS modules of DkxG, H, N, and I are insufficient to accomplish the 5–8 cycles of chain extension required to generate the observed set of polyenes. This finding suggests that at least one PKS module operates repeatedly, a variant on standard PKS biochemistry that is known from several other myxobacterial and *Streptomyces* systems (Olano et al., 2003; He and Hertweck, 2003; Wenzel and Müller, 2007; Tatsuno et al., 2007). Although in principle multiple modules may act repeatedly, in all systems characterized to date, only a single module iterates (Arakawa et al., 2005; Olano et al., 2003; He and Hertweck, 2003; Gaitatzis et al., 2002; Wenzel et al., 2005). As judged by the relative metabolite yields in DK1050 (Figure 1), iteration most often occurs twice, though a third chain extension is also common. Theoretically, any of subunits DkxG, DkxH, DkxN, and DkxI could act iteratively, because they include the appropriate complement of reductive activities to generate a double bond, and the AT domain in each case is predicted to show specificity for malonyl-CoA (Table 3; Haydock et al., 1995; Yadav et al., 2003). However, a significant number of the DKxanthenes generated by both strains incorporate methylmalonate as an extender unit during the third chain extension cycle. The simplest explanation is that the PKS module of DkxG catalyzes this round of chain extension, using alternatively methylmalonate and malonate as building blocks. Indeed, sequence analysis shows that the specificity motifs in the AT domains of DkxG diverge most significantly from the consensus sequence for malonate-selective domains (Table 3).

To support this hypothesis, we mutated the RAAH motif (residues 198–201) of the DkxG AT domain to that characteristic of malonate-specific AT domains (HAFH) (Del Vecchio et al., 2003) using double homologous recombination. Although this change almost completely abolished DKxanthene production (3% of wild-type), we detected an approximately 2-fold increase (and up to 5-fold in single experiments, presumably due to natural fluctuation in production) in the yield of derivatives incorporating malonate instead of methylmalonate (wild-type, DKxanthene −534:DKxanthene −520 = 10:1; mutant PMAT_G, 5:1), supporting the idea that the observed sequence divergence underlies the promiscuity of the AT domain. Similarly, the final polyketide extender unit incorporated into the DKxanthenes is always methyl-malonate. This observation suggests that DkxI catalyzes this single round of chain extension, despite its predicted preference for malonate (Table 3). Taken together, these data implicate either or both of DkxH or DkxN as the iteratively acting module(s).

However, consideration of the nonlinear cluster architecture implicates DkxN as the iterative module and suggests a possible basis for the high level of stuttering. One plausible explanation for the positioning of *dkxN* within the locus is that the gene was acquired by horizontal transfer, because the closest homologs of *dkxN* were identified in species other than *M. xanthus* (data not shown). If the evolutionary integration of DkxN into the pathway is not complete, then docking interactions with both its upstream and downstream partners may be inefficient. In the absence of rapid chain transfer between the subunits, intramodular back transfer of the intermediates from the ACP to the KS domains could become competitive, leading to repetitive chain extension. According to this model, the introduction of DkxN between subunits DkxG and DkxH would lead to iteration both by the PKS module of DkxG (giving rise to DKxanthenes −548 and −574 in *M. xanthus* DK1622), and by module DkxN itself (to yield the remaining metabolites in both strains). Direct experimental support

**Table 3. Active Site, Underlined, and Additional Conserved Residues that Correlate with Domain Specificity in DKxanthene AT Domains from *M. xanthus* DK1622 (DK) and *S. aurantiaca* DW4/3-1 (DW)**

| Domain | 11 | 63 | 90 | 91 | 92 | 93 | 94 | 117 | 200 | 201 | 231 | 250 | 255 | 15 | 58 | 59 | 60 | 61 | 62 | 70 | 72 | 197 | 198 | 199 |
|---|---|---|---|---|---|---|---|---|---|---|---|---|---|---|---|---|---|---|---|---|---|---|---|---|
| DkxG_DK | Q | Q | G | H | S | T | G | R | **A** | **H** | M | Q | V | Y | Q | L | D | Y | A | E | A | P | **R** | **A** |
| DkxG_DW | Q | Q | G | H | S | T | G | R | **A** | **H** | M | Q | V | Y | Q | F | D | Y | A | E | A | P | **R** | **A** |
| DkxH_DK | Q | Q | G | H | S | V | G | R | **F** | **H** | L | H | V | Y | E | T | R | Y | T | E | A | S | **H** | **A** |
| DkxH_DW | Q | Q | G | H | S | V | G | R | **F** | **H** | L | H | V | Y | E | T | R | Y | T | E | A | S | **H** | **A** |
| DkxI_DK | Q | Q | G | H | S | L | G | R | **F** | **H** | L | Q | V | R | D | T | R | H | A | E | A | S | **Y** | **A** |
| DkxI_DW | Q | Q | G | H | S | L | G | R | **F** | **H** | L | H | V | Q | D | T | R | N | A | E | A | P | **H** | **A** |
| DkxN_DK | Q | Q | G | H | S | V | G | R | **F** | **H** | L | H | V | W | E | T | G | F | T | E | A | S | **H** | **A** |
| DkxN_DW | Q | Q | G | H | S | V | G | R | **F** | **H** | L | H | V | W | E | T | G | Y | T | E | A | S | **H** | **A** |
| DkxN'_DW | Q | L | G | S | G | T | G | L | **M** | **S** | V | S | S | P | A | P | G | I | A | Q | G | P | **H** | **A** |

Consensus active site residues for methylmalonate- and malonate-specific AT domains are QQGHS[QMI]GRSHT[NS]V and QQGHS[LVIFAM]GR-[FP]H[ANTGEDS][NHQ]V, respectively (Yadav et al., 2003). Residues in bold correspond to a shorter sequence motif that correlates with specificity for methylmalonate (YASH) or malonate (HAFH) (Del Vecchio et al., 2003; Haydock et al., 1995).

for this hypothesis is provided by analysis of the AT mutant of DkxG. In wild-type cultures of *M. xanthus*, DKxanthene −548 (incorporating a methyl group at $R^2$) is produced at similar levels to DKxanthene −534 (incorporating a hydrogen at $R^2$). However, in the AT mutant in which DKxanthene −534 is present, production of DKxanthene −548 relative to DKxanthene 534 is reduced by at least 2-fold (i.e., to essentially background levels), on the basis of analysis of extracts in quintuplicate. Thus, the mutation to alter the AT specificity of DkxG affected extender unit selection in two successive rounds of chain extension (see above), consistent with the iterative action of the module. The fact that metabolites exhibiting a methyl group at $R^2$ are not observed in *S. aurantiaca* (Figure 1A) suggests that docking between DkxG and DkxN in this strain may be more effective. In addition, some as yet unidentified structural feature of DkxN may favor iterative behavior, because the biosynthesis of every metabolite requires at least one iteration. A model invoking inefficient docking between a "single use" and an inherently iterative module may also apply to the biosynthesis of the myxochromides in *S. aurantiaca* DW4/3-1 (Wenzel et al., 2005), in which the chain length of the polyene functionality is variable. Despite the appeal of this proposal, we cannot at present exclude an alternative mechanism in which DkxH is the iterative module, or indeed in which both DkxN and DkxH act repeatedly.

To attempt to provide further experimental support for this mechanism, the conserved NADPH-binding motif (GxGxxG) of each KR domain within subunits DkxG, H, I, and N was disrupted by point mutation. We hoped that the presence of several unreduced keto groups in the products of one or more mutants would confirm which module or modules was iterating. Disappointingly, all of the mutations completely abolished production of the DKxanthenes (Figure 1B, mutant PMΔRF_I). We also mutated the malonate-specific HAFH motif (Haydock et al., 1995) of the DkxH AT domain to the methymalonate-specific YASH, anticipating that novel methyl branching within the products would allow us to pinpoint the location of the subunit within the assembly line. However, the product profile relative to wild-type was unchanged, although overall metabolite yields dropped to approximately 10% of the wild-type level (Figure 1B). Therefore, the identity of the highly iterating module (DkxN, DkxH, or both) remains to be demonstrated, as do the factors controlling the number of times chain extension is repeated. Experiments to address these issues are ongoing in the laboratory.

By use of HPLC-MS, we routinely detected DKxanthene metabolites that appeared as double peaks. These data suggest that each DKxanthene is present in extracts as a mixture of *cis* and *trans* isomers. The final double bond geometry is assumed to arise from DH-catalyzed dehydration of a β-hydroxy precursor. Comparison by Caffrey (2003) of KR domains from a large number of PKS systems revealed sequence motifs which correlate with the two alternative directions of ketoreduction, termed A- and B-side selective (Baerga-Ortiz et al., 2006; O'Hare et al., 2006). Assuming that dehydration occurs by *syn* elimination of water, B-side reduction predicts a final *trans* double bond geometry. All KR domains within the DKxanthene cluster bear the hallmark motifs of B-selective enzymes, an observation that predicts that the native DKxanthenes should exhibit exclusively *trans* double bonds. The presence of *cis* isomers is therefore ascribed to (light-induced) isomerization under the work-up conditions.

The final round of chain extension occurs on the NRPS subunit DkxJ, with incorporation into the intermediate of asparagine, followed by TE-catalyzed release of the intermediates as their free acids (Figure 3). The 10-residue specificity motif (DGTKVGEV) of the DkxJ A domain, although consistent with a preference for Asn, shows deviations from the canonical code (Stachelhaus et al., 1999; Challis et al., 2000). This observation encouraged us to attempt to alter the domain's specificity by mutating one or two residues to yield, respectively, the motifs associated with activation of aspartate (DLTK(IV)G(AH)(VI); mutant PMAsp) and tyrosine (D(GA)(TL)(IG)T(AG)EV; mutant PMTyr). However, the PMAsp mutant failed to produce novel analogs of the DKxanthenes, whereas biosynthesis in the PMTyr mutant was completely abolished. This result is perhaps not surprising, because attempts to alter the specificity of A domains by site-directed mutagenesis have produced modest results, likely because of the strong proofreading activity of the condensation domains at their acceptor sites (Lautru and Challis, 2004). Alternatively or in addition, the TE was unable to recognize the novel amino acids. The intolerance of the DKxanthene assembly line to changes in both PK and NRP extender units contrasts dramatically with the ability of subunits DkxI and DkxJ to recognize

a variety of chain extension intermediates of differing lengths. Taken together, these data imply that evolution has selected for specific structural features (e.g., an unfunctionalized polyene, the terminal Asn) in the DKxanthenes, suggesting their importance for the biological activity of the metabolites.

The cluster also contains a discrete (or type II) TE activity encoded by *dkxO*. Type II TEs are postulated to regenerate stalled assembly lines through hydrolytic release of misacylated (Heathcote et al., 2001; Schwarzer et al., 2002), and in the case of NRPS, mis-aminoacylated (Yeh et al., 2004) substrates from the integral carrier proteins. Consistent with these proposed functions, inactivation of *dkxO* by homologous recombination reduced the production of the DKxanthenes to 5% of wild-type levels.

### Post-Assembly Line Elaboration of the DKxanthenes

*M. xanthus* DK1622 produces 7 derivatives that are not present in *S. aurantiaca* DW4/3-1. The majority of these metabolites arise from hydroxylation at the β-position of Asn (Figure 1B), which is assumed to occur following release of the chain from DkxJ. In addition, three hydroxylated metabolites (DKxanthene −548, −574, and −586) that do not have nonhydroxylated counterparts in either of the strains are present in *M. xanthus*. As discussed previously, compounds −548 and −574 may arise from stuttering of module DkxG within the *M. xanthus* pathway. Consistent with these observations, the gene cluster in *M. xanthus* contains a putative FAD-binding monooxygenase, DkxD, which is absent from the biosynthetic locus in DW4/3-1. However, several attempts to demonstrate the function of DkxD as an asparagine hydroxylase, including deletion and selective inactivation of the gene, failed. Deletion of gene *dkxC* (which is also absent in *S. aurantiaca*) was successful but did not alter DKxanthene production in *M. xanthus* (data not shown), suggesting that it is not involved in the pathway or is complemented by a gene located elsewhere on the chromosome. Both clusters also contain the gene *dkxK*, which encodes a putative patatin-like phospholipase. A function for such an enzyme in the pathway is not obvious, but intriguingly, genes for patatin-like proteins are present in other biosynthetic gene clusters from myxobacteria, such as that for tubulysin biosynthesis in *Angiococcus disciformis* (Sandmann et al., 2004). Experiments to explore possible functions for DkxK are under way.

## SIGNIFICANCE

**A feature that distinguishes many myxobacterial megasynthetase systems from their *Streptomyces* counterparts is the generation of natural product families, some of which are large. We have identified five DKxanthene mixed polyketide-nonribosomal polypeptide metabolites in the myxobacterium *Stigmatella aurantiaca* that differ not only in the length of the central polyene chromophore but also in the degree of methyl branching. A further eight structures have been characterized from *Myxococcus xanthus*, many of which incorporate a hydroxylated asparagine residue. Our analysis of the gene clusters from these two microorganisms has begun to shed light on the mechanistic basis for this "diversity-oriented" biosynthesis, which may be relevant to additional PKS-NRPS pathways in myxobacteria and other microbes. In DKxanthene biosynthesis, the 5–8 double bonds likely derive from different levels of iteration by one or more PKS modules within the mixed PKS-NRPS synthetase. This variable "stuttering" of chain extension may be induced by the presence of at least one suboptimal intersubunit interface, so that intramodular back transfer of intermediates becomes kinetically competitive with intermodular chain transfer. An additional level of diversity is introduced by an AT domain that recruits both malonate and methylmalonate as building blocks for chain extension. Despite the inherent tolerance of this system to structural variation, our attempts deliberately to alter the metabolites by genetic engineering met with limited success. These data demonstrate that both tight substrate specificity and relative promiscuity can coexist within a single multienzyme assembly line and point to the importance of particular functionalities in conferring bioactivity on the metabolites.**

## EXPERIMENTAL PROCEDURES

### General Materials and Methods

Chemical reagents were obtained from Sigma-Aldrich and used without further purification. All solvents were purified by distillation. Reaction progress was monitored by TLC using 0.2 mm precoated plastic sheets (Polygram Sil G/$UV_{245}$; Macherey-Nagel). Column chromatography was performed using Merck Kieselgel 60. NMR spectra were recorded on a Bruker AMX400 spectrometer with TMS as internal standard. Coupling constants $^{3}J_{H,H}$ are given in Hz.

### Strains and Growth Conditions

Wild-type and mutant strains of *Myxococcus xanthus* DK1050 (Ruiz-Vazquez and Murillo, 1984) were grown at 30°C in CTT medium (Kroos et al., 1986). *S. aurantiaca* DW4/3-1 (Qualls et al., 1978) and its mutants were grown at 30°C in tryptone or tryptone-starch medium (Silakowski et al., 1998). *E. coli* strains TOP10 (Invitrogen) and DH10B were grown at 37°C in Luria-Bertani (LB) medium (Sambrook et al., 1989). When required, kanamycin was used at 40 μg $ml^{-1}$.

### Analysis of DKxanthene Production

*M. xanthus* and *S. aurantiaca* cells were cultivated in 30 ml CTT or tryptone medium, respectively, harvested after three days of growth, and extracted with ethyl acetate:methanol (1:4). The extracts were concentrated in vacuo and then analyzed by use of HPLC-MS (Agilent 1100 series HPLC coupled to a Bruker HCT plus mass spectrometer set to positive ionization mode). To quantify metabolite yields, peaks corresponding to specific DKxanthenes in the extracted ion chromatograms were integrated, and the yield of the respective metabolites was calculated with respect to the cell density by dividing the total amount of DKxanthene by the optical density. Compound pairs DKxanthene −520/−534, and −534/−548 were chosen as the representatives of metabolites that incorporate zero to two methyl groups at positions $R^1$ and $R^2$. To compare production by *M. xanthus* wild-type and mutant strains PMAT_DkxG and PMAT_DkxH, we determined the production ratios of DKxanthene −534 to DKxanthene −520 and DKxanthene −534 to DKxanthene −548, respectively.

### Identification of the DKxanthene Biosynthetic Gene Cluster in *S. aurantiaca* DW4/3-1

Two contiguous sequences of *S. aurantiaca* were identified by sequence comparison with the DKxanthene gene cluster of *M. xanthus* DK1622, which spanned genes *dkxA* to the beginning of *dkxS*, and the end of *dkxS* to *dkxO*, respectively. The KS domain of the NRPS/PKS-encoding gene *dkxG* was inactivated, leading to the abolishment of DKxanthene production (see below). The missing sequence information for gene *dkxS* was obtained by PCR with primers PKSx2_550f (5′-CCCCCGTGAGGAGTTGAC-3′) and PKSx2_551r (5′-GTGCGCAGCTCGTGGACA-3′) using *S. aurantiaca* DW4/3-1 genomic

DNA. The resulting 400 bp fragment was cloned into plasmid pCR2.1-TOPO and sequenced (MWG Biotech AG). The sequence has been deposited in the EMBL database under accession code BN001209.

### Annotation of the DKxanthene Biosynthetic Gene Clusters and Assignment of Domain Functions

Sequence information for the DKxanthene biosynthetic gene clusters in *M. xanthus* DK1622 was obtained from TIGR (http://www.tigr.org/tdb). Protein and domain analysis were performed using the NCBI protein blast (http://www.ncbi.nlm.nih.gov/BLAST/) as well as a NRPS/PKS-analysis program (http://www.tigr.org/jravel/nrps/).

### Inactivation of *dkxA*, *dkxN*, and *dkxO* in *M. xanthus* DK1050, and *dkxG* in *S. aurantiaca* DW4/3-1

Genes *dkxA*, *dkxN*, and *dkxO* were disrupted in *M. xanthus* DK1050. An internal fragment of each gene was amplified from *M. xanthus* genomic DNA by PCR using *Taq* polymerase (Fermentas) (for oligonucleotide sequences see Table S1). To inactivate *dkxG* in *S. aurantiaca* DW4/3-1, an 824 bp internal fragment of *dkxG* was amplified using HotStarTaq DNA polymerase (QIAGEN). All PCR fragments were cloned into plasmid pCR2.1-TOPO, and the resulting plasmids (Table S1) were purified from *E. coli* TOP10 (Invitrogen) or DH10B cells and introduced into *M. xanthus* DK1050 or *S. aurantiaca* DW4/3-1, respectively, by electroporation (Gorski and Kaiser, 1998). Mutants were tested for kanamycin resistance and were genetically verified by PCR using a plasmid-specific primer pair and two primers that bind in the genome outside the inactivation fragment (Jakobsen et al., 2004).

### Inactivation of Ketoreductase Domains of *dkxG*, *dkxH*, *dkxI*, and *dkxN* in *M. xanthus* DK1050

A 1200 bp fragment of each ketroreductase domain incorporating the desired mutation in the NADPH-binding motif was amplified by overlap extension PCR (Higuchi et al., 1988) using Phusion polymerase (Finnzymes). The PCR products were subsequently digested (*Sac*I/*Xba*I) and cloned into plasmid pSWU41, which was previously digested with both *Sac*I and *Xba*I; pSWU41 contained a neomycin phosphotransferase (*nptII*) and levansucrose (*sacB*) gene cassette (Wu and Kaiser, 1996). (Details of plasmid construction and oligonucleotide sequences are provided in Table S1.) The final plasmids—pDkxG_KR, pDkxH_KR, pDkxI_KR and pDkxN_KR, respectively—were introduced into *M. xanthus* DK1050 by electroporation, and clones were selected for kanamycin resistance. In each case, correct integration into the genome was confirmed by PCR. To obtain double homologous recombination, single crossover mutants were grown in CTT medium without kanamycin and were repeatedly recultured in fresh medium. Aliquots were regularly drawn from the culture broth, mixed with CTT soft agar containing 5% sucrose, and plated onto CTT agar plates containing 5% sucrose. Single clones were transferred onto fresh CTT agar plates containing either sucrose or kanamycin. Colonies that grew only on sucrose agar were analyzed genetically and tested for secondary metabolite production. Chromosomal DNA was obtained from the potential mutants, and the target sequence in the KR domains was amplified by PCR. The PCR fragment was cloned into plasmid pCR2.1-TOPO and was sequenced to confirm the presence of the desired mutation. Mutants exhibiting the desired genotype were designated PMΔRF_G, PMΔRF_H, PMΔRF_I, and PMΔRF_N for mutations in the KR domains of *dkxG*, *dkxH*, *dkxI*, and *dkxN*, respectively.

### Alteration of the Specificity-Conferring Residues of the AT Domains of *dkxG* and *dkxH* in *M. xanthus* DK1050

The specificity-conferring residues (Del Vecchio et al., 2003; Yadav et al., 2003) of all DKxanthene AT domains were identified. Target residues in the AT domains of *dkxG* and *dkxH* domains were then mutated using a double crossover strategy, as described above. In both cases, a fragment containing the mutated residues was generated by overlap extension PCR. The *dkxG* fragment was digested with *Sac*I/BamHI, whereas the *dkxH* fragment was digested with *Sac*I/*Xba*I, and then both fragments were cloned into previously digested pSWU41 (oligonucleotide sequences are provided in Table S1). Transformation, cultivation, and screening for single crossover and double crossover mutants was performed as described above. Mutants bearing the desired genotype were designated PMAT_G and PMAT_H, respectively.

### Attempted Alteration of the Substrate Specificity of the A Domain of *dkxJ* in *M. xanthus* DK1050

The specificity-conferring "code" of the DkxJ A domain-binding pocket was identified by sequence analysis (Challis et al., 2000; Stachelhaus et al., 1999). An E322A mutation was introduced to attempt to switch the specificity from Asn to Asp, whereas two mutations (K278G and V299T) were made in order to switch the specificity to Tyr. In each case, an A domain fragment encompassing the mutations was generated by overlap-extension PCR, and the resulting ~1200 bp fragment was cloned into plasmid pSWU41, leading to constructs pDkxJ_Asp and pDkxJ_Tyr, respectively (oligonucleotide sequences are provided in Table S1). Transformation, cultivation, and screening for single and double crossover mutants was performed as described above. Mutants with the desired genotype were designated PMAsp and PMTyr, respectively.

### Preparation of *N*-Acetyl-*S*-Pyrrolyl-2-Carboxylcysteamine

Pyrrol-2-carboxylic acid (1.11 g, 10 mmol), *N*-acetylcysteamine (1.19 g, 10 mmol), and 4-dimethylaminopyridine (122 mg, 1 mmol) were dissolved in dry $CH_2Cl_2$ (30 ml) and cooled on ice. A solution of *N*, *N*′-dicyclohexylcarbodiimide (2.16 g, 10 mmol) in dry $CH_2Cl_2$ (20 ml) was added drop-wise. The reaction mixture was stirred at room temperature over night. The precipitate (*N*, *N*′-dicyclohexylurea) was removed by filtration, and the filtrate was concentrated to dryness. The residue was purified by column chromatography on silica gel using hexane/ethyl acetate to yield pure *N*-acetyl-*S*-pyrrolyl-2-carboxylcysteamine (Pyrrolyl-2-carboxyl-SNAC) (1.95 g, 92%). $^1$H NMR (400 MHz, $CDCl_3$): $\delta$ = 1.97 (s, 3H, $CH_3$), 3.18 (t, 2H, $J$ = 6.3, $CH_2$), 3.50 (t, 2H, $J$ = 6.2, $CH_2$), 6.19 (br s, 1H, NH), 6.26–6.29 (m, 1H, CH), 7.01–7.06 (m, 2H, 2 × CH). $^{13}$C NMR (100 MHz, $CDCl_3$): $\delta$ = 23.2 ($CH_3$), 27.7 ($CH_2$), 40.0 ($CH_2$), 110.9 (CH), 115.8 (CH), 124.3 (CH), 129.8 (C), 170.5 (CONH), 181.6 (COS).

### Feeding of Pyrrolyl-2-Carboxyl-SNAC to Mutant PM1284

Pyrrolyl-2-carboxyl-SNAC (10 mg) was added to a CTT culture of PM1284 (25 ml), at early logarithmic phase. Cultivation, extraction, and analysis by HPLC-MS were performed as described above.

## SUPPLEMENTAL DATA

Supplemental data include six tables and one figure and are available online at http://www.chembiol.com/cgi/content/full/15/8/771/DC1/.

## ACKNOWLEDGMENTS

Research in R.M.'s laboratory was supported by grants from the Bundesministerium für Bildung und Forschung (BMB+F) and the Deutsche Forschungsgemeinschaft (DFG). K.J.W. is an Alexander von Humboldt Research Fellow.

Received: March 17, 2008
Revised: June 4, 2008
Accepted: June 9, 2008
Published: August 22, 2008

## REFERENCES

Altschul, S.F., Madden, T.L., Schaffer, A.A., Zhang, J.H., Zhang, Z., Miller, W., and Lipman, D.J. (1997). Gapped BLAST and PSI-BLAST: a new generation of protein database search programs. Nucleic Acids Res. *25*, 3389–3402.

Arakawa, K., Sugino, F., Kodama, K., Ishii, T., and Kinashi, H. (2005). Cyclization mechanism for the synthesis of macrocyclic antibiotic lankacidin in *Streptomyces rochei*. Chem. Biol. *12*, 249–256.

Avadhani, M., Geyer, R., White, D.C., and Shimkets, L.J. (2006). Lysophosphatidylethanolamine is a substrate for the short-chain alcohol dehydrogenase SocA from *Myxococcus xanthus*. J. Bacteriol. *188*, 8543–8550.

Baerga-Ortiz, A., Popovic, B., Siskos, A.P., O'Hare, H.M., Spiteller, D., Williams, M.G., Campillo, N., Spencer, J.B., and Leadlay, P.F. (2006). Directed mutagenesis alters the stereochemistry of catalysis by isolated ketoreductase domains from the erythromycin polyketide synthase. Chem. Biol. *13*, 277–285.

Burchard, R.P., Burchard, A.C., and Parish, J.H. (1977). Pigmentation phenotype instability in *Myxococcus xanthus*. Can. J. Microbiol. *23*, 1657–1662.

Butcher, R.A., Schroeder, F.C., Fischbach, M.A., Straight, P.D., Kolter, R., Walsh, C.T., and Clardy, J. (2007). The identification of bacillaene, the product of the PksX megacomplex in *Bacillus subtilis*. Proc. Natl. Acad. Sci. USA *104*, 1506–1509.

Caffrey, P. (2003). Conserved amino acid residues correlating with ketoreductase stereospecificity in modular polyketide synthases. ChemBioChem *4*, 654–657.

Challis, G.L., Ravel, J., and Townsend, C.A. (2000). Predictive, structure-based model of amino acid recognition by nonribosomal peptide synthetase adenylation domains. Chem. Biol. *7*, 211–224.

Chen, X.H., Vater, J., Piel, J., Franke, P., Scholz, R., Schneider, K., Koumoutsi, A., Hitzeroth, G., Grammel, N., Strittmatter, A.W., et al. (2006). Structural and functional characterization of three polyketide synthase gene clusters in *Bacillus amyloliquefaciens* FZB 42. J. Bacteriol. *188*, 4024–4036.

Del Vecchio, F., Petkovic, H., Kendrew, S.G., Low, L., Wilkinson, B., Lill, R., Cortés, J., Rudd, B.A., Staunton, J., and Leadlay, P.F. (2003). Active-site residue, domain and module swaps in modular polyketide synthases. J. Ind. Microbiol. Biotechnol. *30*, 489–494.

Fischbach, M.A., and Clardy, J. (2007). One pathway, many products. Nat. Chem. Biol. *3*, 353–355.

Frank, B., Knauber, J., Steinmetz, H., Scharfe, M., Blöcker, H., Beyer, S., and Müller, R. (2007). Spiroketal polyketide formation in *Sorangium*: identification and analysis of the biosynthetic gene cluster for the highly cytotoxic spirangienes. Chem. Biol. *14*, 221–233.

Gaitatzis, N., Silakowski, B., Kunze, B., Nordsiek, G., Blöcker, H., Höfle, G., and Müller, R. (2002). The biosynthesis of the aromatic myxobacterial electron transport inhibitor stigmatellin is directed by a novel type of modular polyketide synthase. J. Biol. Chem. *277*, 13082–13090.

Garneau, S., Dorrestein, P.C., Kelleher, N.L., and Walsh, C. (2005). Characterization of the formation of the pyrrole moiety during clorobiocin and coumermycin A1 biosynthesis. Biochemistry *44*, 2770–2780.

Goldman, B.S., Nierman, W.C., Kaiser, D., Slater, S.C., Durkin, A.S., Eisen, J., Ronning, C.M., Barbazuk, W.B., Blanchard, M., Field, C., et al. (2006). Evolution of sensory complexity recorded in a myxobacterial genome. Proc. Natl. Acad. Sci. USA *103*, 15200–15205.

Gorski, L., and Kaiser, D. (1998). Targeted mutagenesis of sigma54 activator proteins in *Myxococcus xanthus*. J. Bacteriol. *180*, 5896–5905.

Hardt, I.H., Steinmetz, H., Gerth, K., Sasse, F., Reichenbach, H., and Höfle, G. (2001). New natural epothilones from *Sorangium cellulosum*, strains So ce90/B2 and So ce90/D13: isolation, structure elucidation, and SAR studies. J. Nat. Prod. *64*, 847–856.

Haydock, S.F., Aparicio, J.F., Molnar, I., Schwecke, T., König, A., Marsden, A.F., Galloway, I.S., Staunton, J., and Leadlay, P.F. (1995). Divergent structural motifs correlated with the substrate specificity of (methyl)malonyl-CoA:acyl carrier protein transacylase domains in the modular polyketide synthases. FEBS Lett. *374*, 246–248.

He, J., and Hertweck, C. (2003). Iteration as programmed event during polyketide assembly; molecular analysis of the aureothin biosynthesis gene cluster. Chem. Biol. *10*, 1225–1232.

He, J., and Hertweck, C. (2005). Functional analysis of the aureothin iterative type I polyketide synthase. ChemBioChem *6*, 908–912.

Heathcote, M.L., Staunton, J., and Leadlay, P.F. (2001). Role of type II thioesterases: evidence for removal of short acyl chains produced by aberrant decarboxylation of chain extender units. Chem. Biol. *8*, 207–220.

Higuchi, R., Krummell, B., and Saiki, R.K. (1988). A general method of *in vitro* preparation and specific mutagenesis of DNA fragments: study of protein and DNA interactions. Nucleic Acids Res. *16*, 7351–7367.

Jakobsen, J.S., Jelsbak, L., Welch, R.D., Cummings, C., Goldman, B., Stark, E., Slater, S., and Kaiser, D. (2004). Sigma54 enhancer binding proteins and *Myxococcus xanthus* fruiting body development. J. Bacteriol. *186*, 4361–4368.

Julien, B., Tian, Z.Q., Reid, R., and Reeves, C.D. (2006). Analysis of the ambruticin and jerangolid gene clusters of *Sorangium cellulosum* reveals unusual mechanisms of polyketide biosynthesis. Chem. Biol. *13*, 1277–1286.

Kaiser, D. (2004). Signaling in myxobacteria. Annu. Rev. Microbiol. *58*, 75–98.

Kopp, F., and Marahiel, M.A. (2007). Macrocyclization strategies in polyketide and nonribosomal peptide biosynthesis. Nat. Prod. Rep. *24*, 735–749.

Kopp, M., Irschik, H., Pradella, S., and Müller, R. (2005). Production of the tubulin destabilizer disorazol in *Sorangium cellulosum*: biosynthetic machinery and regulatory genes. ChemBioChem *6*, 1277–1286.

Kroos, L., Kuspa, A., and Kaiser, D. (1986). A global analysis of developmentally regulated genes in *Myxococcus xanthus*. Dev. Biol. *117*, 252–266.

Krug, D., Zurek, G., Revermann, O., Vos, M., Velicer, G.J., and Müller, R. (2008). Discovering the hidden secondary metabolome of *Myxococcus xanthus*: a study of intraspecific diversity. Appl. Environ. Microbiol. *74*, 3058–3068.

Kuner, J.M., and Kaiser, D. (1982). Fruiting body morphogenesis in submerged cultures of *Myxococcus xanthus*. J. Bacteriol. *151*, 458–461.

Laue, B.E., and Gill, R.E. (1994). Use of a phase variation-specific promoter of *Myxococcus xanthus* in a strategy for isolating a phase-locked mutant. J. Bacteriol. *176*, 5341–5349.

Laue, B.E., and Gill, R.E. (1995). Using a phase-locked mutant of *Myxococcus xanthus* to study the role of phase variation in development. J. Bacteriol. *177*, 4089–4096.

Lautru, S., and Challis, G.L. (2004). Substrate recognition by nonribosomal peptide synthetase multienzymes. Microbiology *150*, 1629–1636.

Meiser, P., Bode, H.B., and Müller, R. (2006). DKxanthenes: novel secondary metabolites from the myxobacterium *Myxococcus xanthus* essential for sporulation. Proc. Natl. Acad. Sci. USA *103*, 19128–19133.

Nowak-Thompson, B., Gould, S.J., and Loper, J.E. (1997). Identification and sequence analysis of the genes encoding a polyketide synthase required for pyoluteorin biosynthesis in *Pseudomonas fluorescens* Pf-5. Gene *204*, 17–24.

Nowak-Thompson, B., Chaney, N., Wing, J.S., Gould, S.J., and Loper, J.E. (1999). Characterization of the pyoluteorin biosynthetic gene cluster of *Pseudomonas fluorescens* Pf-5. J. Bacteriol. *181*, 2166–2174.

O'Hare, H.M., Baerga-Ortiz, A., Popovic, B., Spencer, J.B., and Leadlay, P.F. (2006). High-throughput mutagenesis to evaluate models of stereochemical control in ketoreductase domains from the erythromycin polyketide synthase. Chem. Biol. *13*, 287–296.

Olano, C., Wilkinson, B., Moss, S.J., Brana, A.F., Mendez, C., Leadlay, P.F., and Salas, J.A. (2003). Evidence from engineered gene fusions for the repeated use of a module in a modular polyketide synthase. Chem. Commun. (Camb). *22*, 2780–2782.

Otsuka, M., Ichinose, K., Fujii, I., and Ebizuka, Y. (2004). Cloning, sequencing, and functional analysis of an iterative type I polyketide synthase gene cluster for biosynthesis of the antitumor chlorinated polyenone neocarzilin in "*Streptomyces carzinostaticus*". Antimicrob. Agents Chemother. *48*, 3468–3476.

Perlova, O., Gerth, K., Hans, A., Kaiser, O., and Müller, R. (2006). Identification and analysis of the chivosazol biosynthetic gene cluster from the myxobacterial model strain *Sorangium cellulosum* So ce56. J. Biotechnol. *121*, 174–191.

Qualls, G.T., Stephens, K., and White, D. (1978). Morphogenetic movements and multicellular development in the fruiting myxobacterium *Stigmatella aurantiaca*. Dev. Biol. *66*, 270–274.

Richter, C.D., Nietlispach, D., Broadhurst, R.W., and Weissman, K.J. (2008). Multienzyme docking in hybrid megasynthetases. Nat. Chem. Biol. *4*, 75–81.

Ruiz-Vazquez, R., and Murillo, F.J. (1984). Abnormal motility and fruiting behavior of *Myxococcus xanthus* bacteriophage-resistant strains induced by a clear-plaque mutant of bacteriophage Mx8. J. Bacteriol. *160*, 818–821.

Sambrook, J., Fritsch, E.F., and Maniatis, T. (1989). Molecular cloning: A laboratory manual (Cold Spring Harbor, NY: Cold Spring Harbor Laboratory Press).

Sandmann, A., Sasse, F., and Müller, R. (2004). Identification and analysis of the core biosynthetic machinery of tubulysin, a potent cytotoxin with potential anticancer activity. Chem. Biol. *11*, 1071–1079.

Schwarzer, D., Mootz, H.D., Linne, U., and Marahiel, M.A. (2002). Regeneration of misprimed nonribosomal peptide synthetases by type II thioesterases. Proc. Natl. Acad. Sci. USA *99*, 14083–14088.

Shimkets, L.J. (1999). Intercellular signaling during fruiting-body development of *Myxococcus xanthus*. Annu. Rev. Microbiol. *53*, 525–549.

Silakowski, B., Ehret, H., and Schairer, H.U. (1998). fbfB, a gene encoding a putative galactose oxidase, is involved in *Stigmatella aurantiaca* fruiting body formation. J. Bacteriol. *180*, 1241–1247.

Silakowski, B., Nordsiek, G., Kunze, B., Blöcker, H., and Müller, R. (2001). Novel features in a combined polyketide synthase/non-ribosomal peptide synthetase: the myxalamid biosynthetic gene cluster of the myxobacterium *Stigmatella aurantiaca* Sga15. Chem. Biol. *8*, 59–69.

Simunovic, V., Zapp, J., Rachid, S., Krug, D., Meiser, P., and Müller, R. (2006). Myxovirescin biosynthesis is directed by hybrid polyketide synthases/nonribosomal peptide synthetase, 3-hydroxy-3-methylglutaryl CoA synthases and *trans*-acting acyltransferases. ChemBioChem *7*, 1206–1220.

Stachelhaus, T., Mootz, H.D., and Marahiel, M.A. (1999). The specificity-conferring code of adenylation domains in nonribosomal peptide synthetases. Chem. Biol. *6*, 493–505.

Tang, L., Ward, S., Chung, L., Carney, J.R., Li, Y., Reid, R., and Katz, L. (2004). Elucidating the mechanism of *cis* double bond formation in epothilone biosynthesis. J. Am. Chem. Soc. *126*, 46–47.

Tatsuno, S., Arakawa, K., and Kinashi, H. (2007). Analysis of modular-iterative mixed biosynthesis of lankacidin by heterologous expression and gene fusion. J. Antibiot. (Tokyo). *60*, 700–708.

Thomas, M.G., Burkart, M.D., and Walsh, C.T. (2002). Conversion of L-proline to pyrrolyl-2-carboxyl-S-PCP during undecylprodigiosin and pyoluteorin biosynthesis. Chem. Biol. *9*, 171–184.

Walsh, C.T. (2008). The chemical versatility of natural-product assembly lines. Acc. Chem. Res. *41*, 4–10.

Walsh, C.T., Chen, H.W., Keating, T.A., Hubbard, B.K., Losey, H.C., Luo, L.S., Marshall, C.G., Miller, D.A., and Patel, H.M. (2001). Tailoring enzymes that modify nonribosomal peptides during and after chain elongation on NRPS assembly lines. Curr. Opin. Chem. Biol. *5*, 525–534.

Walsh, C.T., Garneau-Tsodikova, S., and Howard-Jones, A.R. (2006). Biological formation of pyrroles: nature's logic and enzymatic machinery. Nat. Prod. Rep. *23*, 517–531.

Weissman, K.J., and Leadlay, P.F. (2005). Combinatorial biosynthesis of reduced polyketides. Nat. Rev. Microbiol. *3*, 925–936.

Weissman, K.J., and Müller, R. (2008a). A brief tour of myxobacterial secondary metabolism. Bioorg. Med. Chem., in press.

Weissman, K.J., and Müller, R. (2008b). Protein-protein interactions in multienzyme megasynthetases. ChemBioChem *9*, 826–848.

Wenzel, S.C., Kunze, B., Höfle, G., Silakowski, B., Scharfe, M., Blöcker, H., and Müller, R. (2005). Structure and biosynthesis of myxochromides S1–3 in *Stigmatella aurantiaca*: evidence for an iterative bacterial type I polyketide synthase and for module skipping in nonribosomal peptide biosynthesis. ChemBioChem *6*, 375–385.

Wenzel, S.C., and Müller, R. (2007). Myxobacterial natural product assembly lines: fascinating examples of curious biochemistry. Nat. Prod. Rep. *24*, 1211–1224.

Wu, S.S., and Kaiser, D. (1996). Markerless deletions of pil genes in *Myxococcus xanthus* generated by counterselection with the *Bacillus subtilis sacB* gene. J. Bacteriol. *178*, 5817–5821.

Xu, H., Wang, Z.X., Schmidt, J., Heide, L., and Li, S.M. (2002). Genetic analysis of the biosynthesis of the pyrrole and carbamoyl moieties of coumermycin A1 and novobiocin. Mol. Genet. Genomics *268*, 387–396.

Yadav, G., Gokhale, R.S., and Mohanty, D. (2003). Computational approach for prediction of domain organization and substrate specificity of modular polyketide synthases. J. Mol. Biol. *328*, 335–363.

Yeh, E., Kohli, R.M., Bruner, S.D., and Walsh, C.T. (2004). Type II thioesterase restores activity of a NRPS module stalled with an aminoacyl-*S*-enzyme that cannot be elongated. ChemBioChem *5*, 1290–1293.